Journal of Alloys and Compounds 792 (2019) 742–749

Contents lists available at ScienceDirect

Journal of Alloys and Compounds

journal homepage: http://www.elsevier.com/locate/jalcom

Compositional tailoring effect on $ZnGa_2O_4$-TiO_2 ceramics for tunable microwave dielectric properties

Xiaochi Lu [a, b], Wenjie Bian [a, b], Bin Quan [c], Zhefei Wang [d], Haikui Zhu [a, b], Qitu Zhang [a, b, *]

[a] College of Materials Science and Engineering, Nanjing Tech University, Nanjing 210009, PR China
[b] Jiangsu Collaborative Innovation Center for Advanced Inorganic Function Composites, Nanjing Tech University, Nanjing 210009, PR China
[c] College of Materials Science and Technology, Nanjing University of Aeronautics and Astronautics, Nanjing 211100, PR China
[d] College of Chemistry and Materials Engineering, Changshu Institute of Technology, Changshu 215500, PR China

ARTICLE INFO

Article history:
Received 9 March 2019
Received in revised form
7 April 2019
Accepted 9 April 2019
Available online 10 April 2019

Keywords:
Gallium oxide
Composite materials
Dielectric properties
Near zero temperature coefficient

ABSTRACT

(1-*x*)$ZnGa_2O_4$-*x*TiO_2 ($x = 0.05–0.20$) composite ceramics were fabricated via traditional solid state method. The experimental and theoretical value of ε_r, τ_f and $Q \times f$ shows similar trend. Tunable microwave dielectric performance was achieved due to the effect of TiO_2, especially for temperature coefficient and quality factor. The large negative temperature coefficient at resonant frequency (τ_f) of $ZnGa_2O_4$ was continuously tailored from negative (−70 ppm/°C) to positive (+13 ppm/°C) $_2$ For practical application, 15 mol% (about 6.9 V%) TiO_2 can adjust τ_f value to near zero. The tailoring effect on quality factor ($Q \times f$) was significant. Due to the smaller $Q \times f$ values of TiO_2, the $Q \times f$ value decreases with the increasing content of TiO_2. The inhomogeneous microstructure results in the increasing difference between calculated and experimented $Q \times f$ value. In addition, compositing TiO_2 with $ZnGa_2O_4$ ceramic not only promote the grain growth but also reduce its sintering temperature from 1400 °C to 1300 °C. The dielectric constant (ε_r) was not significant affected by TiO_2, only varied from 10.8 to 12.7. The ε_r value of 12.3, $Q \times f$ value of 73,000 GHz (at 11.8 GHz) and τ_f value of +3 ppm/°C were achieved for 0.85$ZnGa_2O_4$-0.15TiO_2, sintered at 1300 °C for 2 h.

1. Introduction

Due to the urgent need of high quality ultra-stable oscillators, ultrahigh-speed wireless local area networks (WLANs), and intelligent transport systems (ITSs), low-K microwave dielectric ceramics with excellent microwave dielectric properties (high $Q \times f$ and near zero τ_f) have caught much attention [1–5].

Al_2O_3 [6], AWO_4 (A = alkaline earth metal ions) [7], R_2BaCuO_5 (R = Y, In) [8], M_2SnO_4 [9,10], M_2SiO_4 [11] and MAl_2O_4 (M = Zn, Mg) [12,13] are six typical low-K microwave dielectric ceramics. Among these, M_2SnO_4, M_2SiO_4 and MAl_2O_4 (M = Zn, Mg) all possess spinel structure with the formula of AB_2O_4. MGa_2O_4 (M = Zn, Mg) [14–17], also a typical spinel ceramic, has been applied in numerous scientific and commercial fields, such as magnetic materials, catalysts, semiconductors, and superconductors. It is a new microwave dielectric ceramic and has attracted the attention since 2013. Although, both of $MgGa_2O_4$ and $ZnGa_2O_4$ are spinel ceramics, they are quite different due to the differences in cation distribution. $ZnGa_2O_4$ is a normal spinel with Zn^{2+} occupying tetrahedral site and Ga^{3+} occupying octahedral site [18]. However, $MgGa_2O_4$ possesses a partial inverse spinel structure with a part of Mg^{2+} entering into octahedral site and the same proportion of Ga^{3+} entering into tetragonal site [19]. Thus, $ZnGa_2O_4$ based materials caught researchers' attention for its simple structure. $ZnGa_2O_4$ ceramics show relative high quality factors over 90,000 GHz, relative low sintering temperature (1385 °C) compared with other single phase low-K ceramics like Al_2O_3 which sintering temperature is over 1800 °C, and wide sintering temperature region [20]. Therefore, $ZnGa_2O_4$ based ceramic materials are considered as good candidates for low-K dielectric ceramic materials.

Many investigations have studied the microwave dielectric performance of $ZnGa_2O_4$ and $ZnGa_2O_4$ based solid solutions [19–26]. Some ions were used to substitute Zn^{2+} or Ga^{3+}, such as Mg^{2+}, Mn^{2+}, Cu^{2+} and Al^{3+} to form solid solutions which proved to be an effectively way to enhance the microwave dielectric properties especially the quality factors ($Q \times f$).

However, the larger negative τ_f value, ~-70 ppm/°C has limited

* Corresponding author. College of Materials Science and Engineering, Nanjing Tech University, Nanjing 210009, PR China.
E-mail address: ngdzqt@163.com (Q. Zhang).

https://doi.org/10.1016/j.jallcom.2019.04.095
0925-8388/

its application. For practical applications, it is required to possess relative low dielectric constant (ε_r), high quality factor ($Q \times f$) and near zero temperature coefficient (τ_f). Thus, compared with improving quality factors, it is more significant for $ZnGa_2O_4$-based ceramics to obtain near zero τ_f value. Usually, the following two ways, substitution with magnetic ion and compositing second phase, are widely accepted to tailor τ_f [27]. In our recent research, the magnetic ion, Mn^{2+}, was used to substitute $ZnGa_2O_4$. It revealed that Mn-substitution can adjust its τ_f value to −12 ppm/°C, however, it is not able to achieve near zero temperature coefficient.

Therefore, it came to us to form composite ceramics to obtain near zero τ_f value. According to the mixture rule [28], material with large negative τ_f, high $Q \times f$ and relative low ε_r is optimal. TiO_2 with large positive τ_f (τ_f = +450 ppm/°C) [28,29] and high $Q \times f$ ($Q \times f$ = 51,000 GHz) supposed to be an effective material which can adjust τ_f value of $ZnGa_2O_4$ ceramic [30]. Furthermore, TiO_2 can adjust τ_f without side reaction, and can reduce sintering temperature at the same time since rutile is a common sintering additive.

In this paper, $ZnGa_2O_4$-TiO_2 composite ceramics were prepared through a conventional solid-state method. The tailoring effect of TiO_2 was systematically investigated, including microwave dielectric properties and sintering behavior.

2. Experiment

2.1. Materials preparation

$ZnGa_2O_4$-TiO_2 composite ceramics were prepared via traditional solid state method. All of the chemicals used in the experiment were analytical grade and used without further purification. $ZnGa_2O_4$ powders were prepared at 1000 °C for 3 h via ZnO, and Ga_2O_3. The prepared powders were then mixed with TiO_2 on the basis of the stoichiometric compositions of (1-x)$ZnGa_2O_4$-$xTiO_2$ (x = 0.05–0.15) denoted as 5T-ZGO, 10T-ZGO, 15T-ZGO and 20T-ZGO. The mixed powders were milled for 8 h with ethanol in polyethylene jars with agate balls in a planetary milling machine. After dried at 100 °C for 24 h, the mixture were calcined at 1000 °C for 2 h 7 wt% polyvinyl alcohol as adhesion agent was added, followed by ceramic powders and pressed into pellets of 13 mm in diameter and 6 mm in thickness under uniaxial pressure ~75 MPa. These pellets were sintered at 1250–1350 °C for 4 h in air with a high-temperature electric furnace (KSX4-16, Allfine, Wuxi, China).

2.2. Measurement

Thermal decomposition was followed by thermo gravimetric analysis (TG-DSC; Model STA 449C, Netzsch, Selb, Germany). The crystalline phases were determined by means of X-ray diffraction (XRD, RigakuD/Max 2500 type, Japan) with Cu Kα radiation. The relative density was evaluated via Archimedes' method. 5 samples were measured for every sintering temperature and give the average density value. Samples for transmission electron microscopy (TEM) analysis were prepared by mechanically disaggregation of the ceramics followed by grinding in an agate mortar. The powders were then suspended in ethanol and dropped onto a carbon-coated copper grid. The high resolution TEM (HRTEM) images and selected-area electron diffraction (SAED) patterns were obtained at 200 kV using transmission electron microscopy (JEM-2100, JEOL). Raman spectra were collected using a Raman spectrometer (HR800, Horiba Labram) and the 514 nm He-Cd laser with 20 mW laser power was used as excitation source. Fourier transform infrared (FT-IR) spectroscopy was performed by NICOLET 5700 (Thermo, America). XPS core-level spectra were taken with an X-ray photoelectron spectrometer (ESCALAB 250, Thermo Fisher, UK). Microstructure evolution and EDS of the obtained ceramics was investigated by a scanning electron microscope (SEM, Hitachi SU8010, Japan). To investigate the microwave dielectric performance, ε_r, $Q \times f$, f_0 and τ_f were detected using cavity resonator method [31] by using Lightwave Component Analyzer (Hewlett Packard 8703A, 1550nm/130 MHz-20GHz), and the resonator size is ϕ36 mm × h25 mm. The temperature coefficient of resonant frequency (τ_f) was calculated in the temperature range from 20 °C to 80 °C.

3. Results and discussion

The TG-DSC curves of ZnO and Ga_2O_3 raw powders are shown in Fig. 1. A strong endothermic peak appeared at around 950 °C, with a small weight loss. This suggests that the formation temperature of $ZnGa_2O_4$ phase is above 950 °C. And through experiments, 1000 °C was selected as the best synthesis temperature. Fig. 2(a–c) shows the sample consisted of nano-plates with a width of 50–100 nm and the length 100–200 nm. Further insight was gained by HRTEM observation on the edge area (marked by A) of the plate, as indicated in Fig. 2(a). It displayed distinct lattice space of 0.29 nm corresponding to a distance of (220) lattice planes (shown in Fig. 2(b)). The corresponding SAED pattern Fig. 2(c) shows the presence of sharp diffraction spots, indicating that the $ZnGa_2O_4$ grains have good crystallinity and possess polycrystalline structure.

Fig. 3(a) shows the XRD patterns of (1-x)$ZnGa_2O_4$-$xTiO_2$ (x = 0.05–0.20) ceramics x, following sintered at 1300 °C for 2 h. Obviously, all the diffraction peaks could be well indexed to spinel structured $ZnGa_2O_4$ (JCPDS No.86-0413) and TiO_2 (JCDPS No.21-1276). Notably, the relative intensity of TiO_2 main diffraction peaks ~27° significantly increases as x increased (shown in Fig. 3(b)). Even at a very low-level TiO_2 content, i.e., $0.95ZnGa_2O_4$-$0.05TiO_2$ (about 2.2 V%), peaks from the TiO_2 phase was observed. In addition, no diffraction peaks can fit with $ZnTiO_3$ or other impurity phases. Therefore, TiO_2 doesn't affect the crystal structure of $ZnGa_2O_4$ or react with $ZnGa_2O_4$. $ZnGa_2O_4$-TiO_2 composite ceramics were successfully prepared via traditional solid state method.

Raman spectrum of $ZnGa_2O_4$-TiO_2 composite ceramics was exhibited in Fig. 4. For rutile, it has three Raman-active modes of multi-proton process (230 cm^{-1}), E_g (445 cm^{-1}) and A_{1g} (610 cm^{-1}) [32] which are marked with "R". And for $ZnGa_2O_4$, two typical modes were T_{2g} (610 cm^{-1}) and A_{1g} (700 cm^{-1}) [33] marked with "Z". It is clearly indicated that both of the rutile and $ZnGa_2O_4$ phases are well preserved in $ZnGa_2O_4$-TiO_2 composite ceramics, which is consistent with XRD patterns.

Fig. 5 shows the FT-IR spectrum of (1-x)$ZnGa_2O_4$-$xTiO_2$ (x = 0.05, 0.10, 0.15, 0.20) composite ceramics. The absorption peaks at around 573 cm^{-1} and 432 cm^{-1} [34] represent the bond vibration of $ZnGa_2O_4$. And the absorption bands at around 700 cm^{-1} in FT-IR

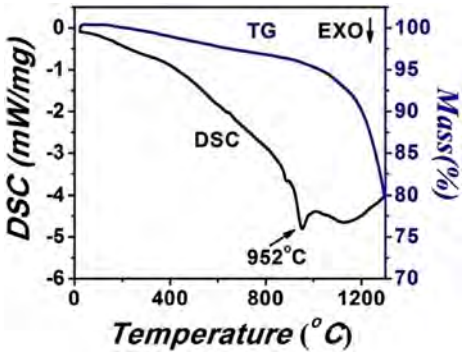

Fig. 1. TG-DSC spectra of $ZnGa_2O_4$ raw materials.

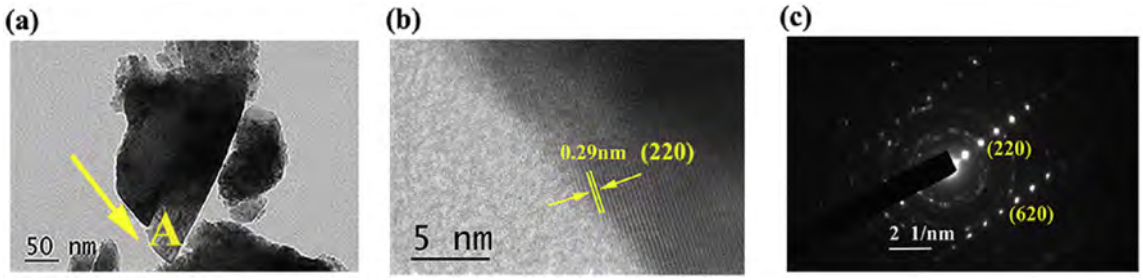

Fig. 2. (a) TEM image, (b) HRTEM image, (c) SAED pattern of $ZnGa_2O_4$ crystal.

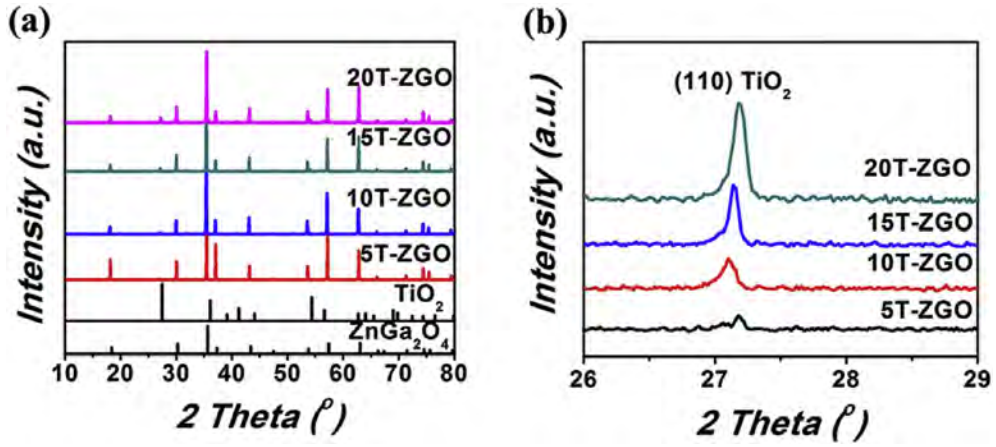

Fig. 3. XRD patterns of (1-*x*)$ZnGa_2O_4$-*x*TiO_2(*x* = 0.05–0.20) composite ceramics sintered at 1300 °C for 2 h in air.

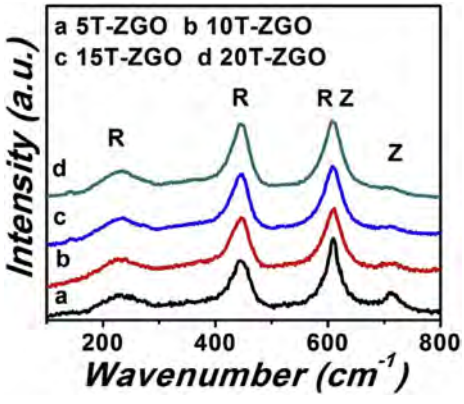

Fig. 4. Raman spectra of (1-*x*)$ZnGa_2O_4$-*x*TiO_2 (*x* = 0.05–0.20) ceramics.

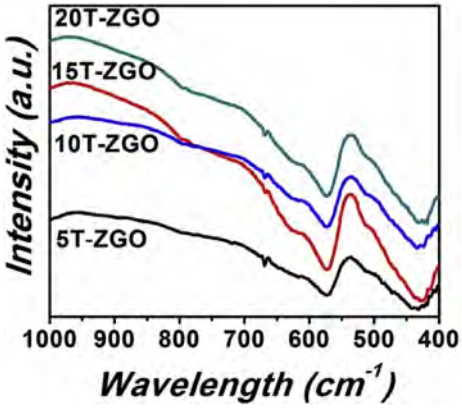

Fig. 5. FT-IR spectrum of (1-*x*)$ZnGa_2O_4$-*x*TiO_2 (*x* = 0.05–0.20) ceramics.

spectrum comes from TiO_2 [35] compared with pure $ZnGa_2O_4$. No obvious peak shift was observed because rutile did not react with or enter into $ZnGa_2O_4$ to change the crystalline structure of spinel structured $ZnGa_2O_4$. And this result in turn proves the XRD data.

To study whether there is any variation in chemical state (especially Ti element), the XPS spectra of $0.15TiO_2$-$0.85ZnGa_2O_4$ composite ceramics were measured and the results are displayed in Fig. 6. Fig. 6(a–d) shows the Zn $2p_{1/2}$, Ga $2p_{3/2}$, O 1s and Ti $2p_{3/2}$, respectively. And through Gaussian–Lorentzian curve fitting, it revealed that there is no other ions but Zn^{2+}, Ga^{3+}, Ti^{4+} and O^{2-} in the compositing ceramics. Therefore, elements in $ZnGa_2O_4$-TiO_2 component ceramic are stable.

To describe the distribution of elements in $ZnGa_2O_4$-TiO_2 composite ceramics, mapping and EDS patterns of $0.85ZnGa_2O_4$-$0.15TiO_2$ are shown in Fig. 7. The three elements: Zn, Ga, Ti exhibit uniform distribution shown in Fig. 7(a–c). EDS pattern confirms the composition of Zn, Ga, and Ti. No obvious phase segregation was observed which means TiO_2 and $ZnGa_2O_4$ phases mixed well.

SEM micrographs of fracture surface of $ZnGa_2O_4$-TiO_2 composite ceramics with various TiO_2 content sintered at 1300 °C are exhibited in Fig. 8. With the increasing of TiO_2 content, the average size increases significantly. Grain growth has been promoted by TiO_2 and exaggerated grain growth behavior is observed due to higher amount of TiO_2. For ceramics of $0.8ZnGa_2O_4$-$0.2TiO_2$, the particles showed a surprising grain growth, properly due to the movement of the grain boundaries through consuming smaller grains. A large number of closed pores were trapped within the

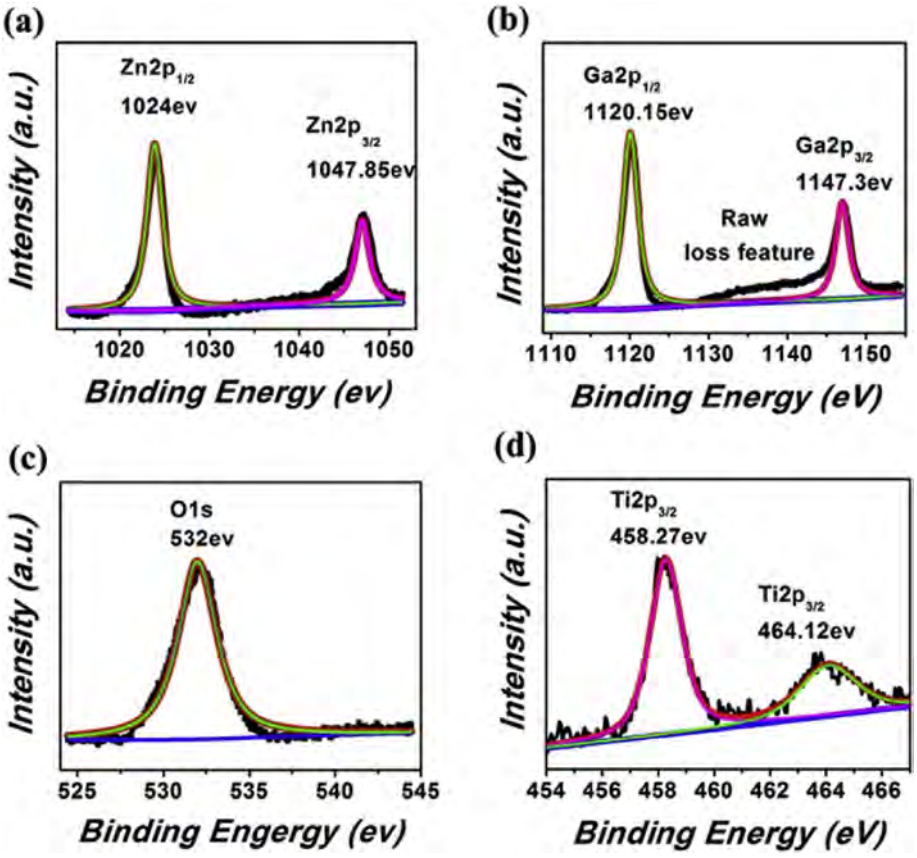

Fig. 6. XPS spectrum of $0.85ZnGa_2O_4$-$0.15TiO_2$ (a) Zn $2p_{1/2}$; (b) Ga $2p_{3/2}$ and Ga $2p_{1/2}$; (c) Ti $2p_{3/2}$; (d) O 1s.

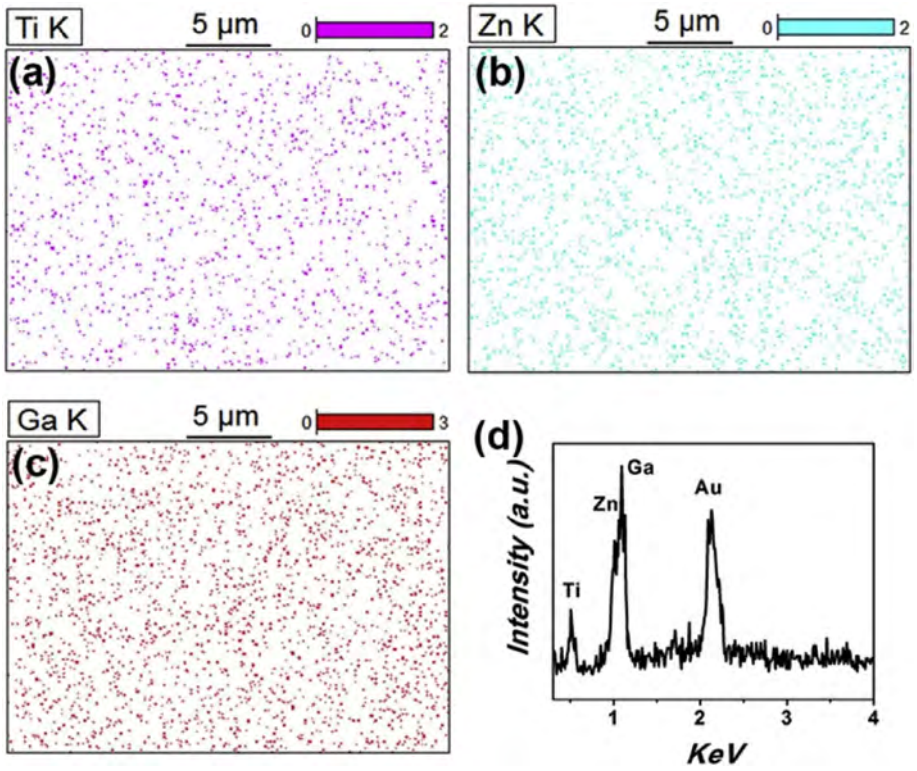

Fig. 7. Energy dispersive spectrometer patterns of $0.85ZnGa_2O_4$-$0.15TiO_2$. (a) Ti distribution, (b) Zn distribution, (c) Ga distribution and (d) EDX pattern.

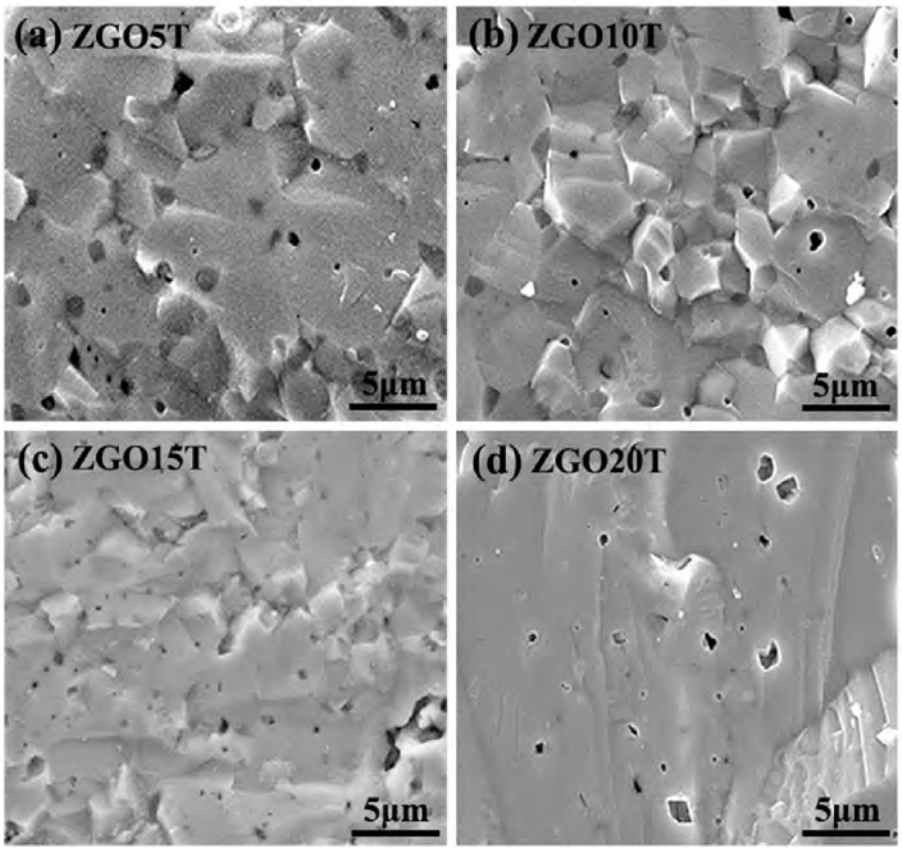

Fig. 8. SEM images of (1-x)$ZnGa_2O_4$-$xTiO_2$($x = 0.05–0.20$) ceramics sintered at 1300 °C for 2 h in air: (a) $x = 0.05$; (b) $x = 0.10$; (c) $x = 0.15$; (d) $x = 0.20$, respectively.

grains. In general, inhomogeneous microstructure may do harm to microwave dielectric properties, especially $Q \times f$.

Fig. 9 shows the bulk and relative density of (1-x)$ZnGa_2O_4$-$xTiO_2$ ($x = 0.05–0.20$) sintered at various temperatures from 1250 °C to 1400 °C for 2 h TiO_2 (5.01 g/cm^3) and $ZnGa_2O_4$ (5.99 g/cm^3) were used to calculated relative density. The maximum bulk and relative density for (1-x)$ZnGa_2O_4$-$xTiO_2$ were achieved at 1300 °C. At this sintering temperature, the relative density is independent of TiO_2 content with almost the same value. Obviously, dense structure is good for the microwave dielectric performance. Therefore, 1300 °C is the optimal sintering temperatures for $ZnGa_2O_4$-TiO_2 composite ceramics.

Fig. 10(a–c) displays the dielectric constant, resonant frequency, and quality factors of $ZnGa_2O_4$-TiO_2 composite ceramics as a function of sintering temperatures. Clearly, the dielectric constant (ε_r) for each composition all shows the same tendency that ε_r increases from 1250 °C to 1300 °C and achieve its highest value at 1300 °C then decreases. ε_r depends on three factors: sample size (shape, diameter and thickness), phase composition and density. As the sample size is almost the same mentioned in the experimental part, the dielectric constant was determined by density and phase composition. For resonant frequency (Fig. 10 (b)), it shows inverse trend as ε_r cause f_0 is dominated by the resonator surroundings, ε_r and the sample size. According to the formula $f_0 \propto 1/(v^* (\varepsilon_r)^{1/2})$ [3],

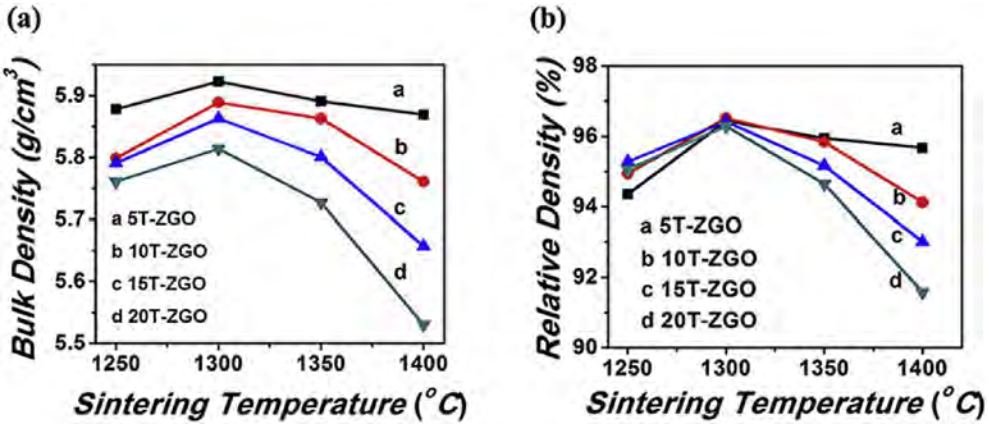

Fig. 9. The bulk and relative densities of $ZnGa_2O_4$-TiO_2 composite ceramics, sintered at various temperatures range from 1250 °C to 1400 °C for 2 h in air.

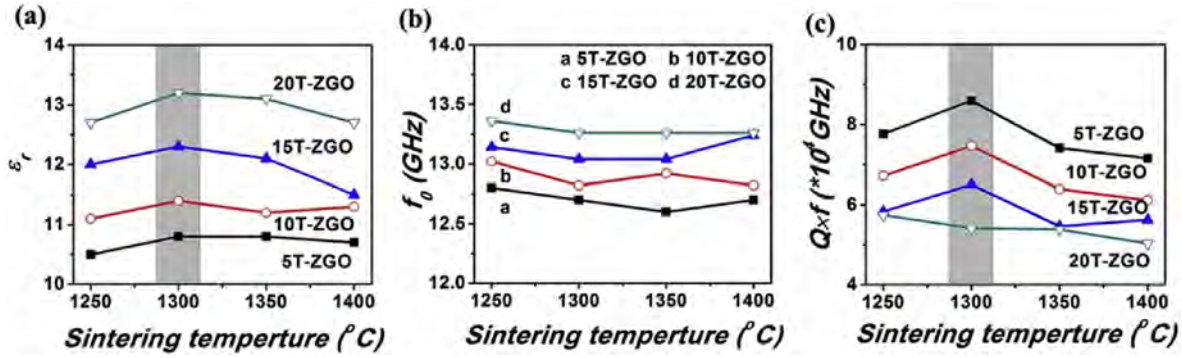

Fig. 10. (a) Dielectric constant (ε_r), (b) resonant frequency (f_0), and (c) quality factor ($Q \times f$) of $ZnGa_2O_4$-TiO_2 composite ceramics as a function of sintering temperatures.

due to the same resonator surroundings and sample size, f_0 only depends on ε_r. Therefore f_0 decreases with the increasing of ε_r. Fig. 10 (c) displays the $Q \times f$ variation of (1-x)$ZnGa_2O_4$-$x$$TiO_2$ ($x = 0.05–0.20$). The $Q \times f$ value significantly changed with sintering temperatures and obtained the highest value for all specimens sintered at 1300 °C. Therefore, 1300 °C is the optimized sintering temperature for ε_r and $Q \times f$ which agrees with the results of the relative density. Obviously, the tailoring effect of TiO_2 on ε_r and $Q \times f$ was remarkable shown in Fig. 10 (a) and (c). ε_r increases from 10.8 to 12.7 with the increasing content of TiO_2. For $Q \times f$, it declined with x increased, to a minimum value of 54,190 GHz (x = 0.20). And this can be ascribed to the lower $Q \times f$ value of TiO_2 compared with $ZnGa_2O_4$, as well as poorer microstructure.

Table 1
List of the composition of $ZnGa_2O_4$-TiO_2 composite ceramics.

Composition\Fraction	x (mol%)	V (%)
5T-ZGO	5	2.2
10T-ZGO	10	4.5
15T-ZGO	15	6.9
20T-ZGO	20	9.5

Table 2
List of microwave dielectric properties of $ZnGa_2O_4$-TiO_2 composite ceramics.

Composition\Properties	ε_r	τ_f (ppm/°C)	$Q \times f$ (GHz)
5T-ZGO	10.8	−23	85,927
10T-ZGO	11.4	−12	74,601
15T-ZGO	12.1	+4.0	65,032
20T-ZGO	12.7	+13	54,190

In order to calculate the theoretical τ_f, ε_r and $Q \times f$, Table 1 transforms the composition of the composite ceramics from mole percent into volume percentage. And Table 2 summarizes the microwave dielectric properties of (1-x)$ZnGa_2O_4$-$x$$TiO_2$ ($x = 0.05–0.20$) fired at 1300 °C for 2 h. Fig. 11(a) exhibits the experimental and theoretical temperature coefficient at resonant frequency of $ZnGa_2O_4$-TiO_2 composite ceramics sintered at 1300 °C. The theoretical τ_f was calculated based on $\tau_f = \nu_1\tau_{f1} + \nu_2\tau_{f2}$, where ν_1, ν_2 are the volume fraction, and τ_{f1}, τ_{f2} are the temperature coefficient of $ZnGa_2O_4$ (−60 ppm/°C) and TiO_2 (+450 ppm/°C), respectively. Notably, there is a strong linear positive correlation between τ_f and TiO_2 content both for experimental and theoretical τ_f. The relative density and microstructure are responsible for the difference between theoretical and experimental τ_f value of $ZnGa_2O_4$-TiO_2 composite ceramics. The τ_f shifted from negative value to positive value with the increasing TiO_2 content $_2$, and samples with composition of 0.85$ZnGa_2O_4$-0.15TiO_2 achieve the near zero τ_f of about 4 ppm/°C. Therefore, 0.85$ZnGa_2O_4$-0.15TiO_2 is the optimal composition for the best comprehensive dielectric performance.

Fig. 11(b) shows the experimental and theoretical dielectric constant of $ZnGa_2O_4$-TiO_2 composite ceramics (sintered at 1300 °C). The theoretical ε_r was calculated based on $\ln\varepsilon_r = \nu_1\ln\varepsilon_{r1} + \nu_2\ln\varepsilon_{r2}$, where ν_1, ν_2 are the volume fraction, and ε_{r1}, ε_{r2} are the dielectric constant of $ZnGa_2O_4$ and TiO_2, respectively. ε_r used in this paper for evaluation of $ZnGa_2O_4$ and TiO_2 is 10 and 100. Notably, there is a strong linear positive correlation between the dielectric constant and TiO_2 content both for experimental and theoretical ε_r. As discussed in τ_f section, the relative density and microstructure are responsible for the difference between theoretical and

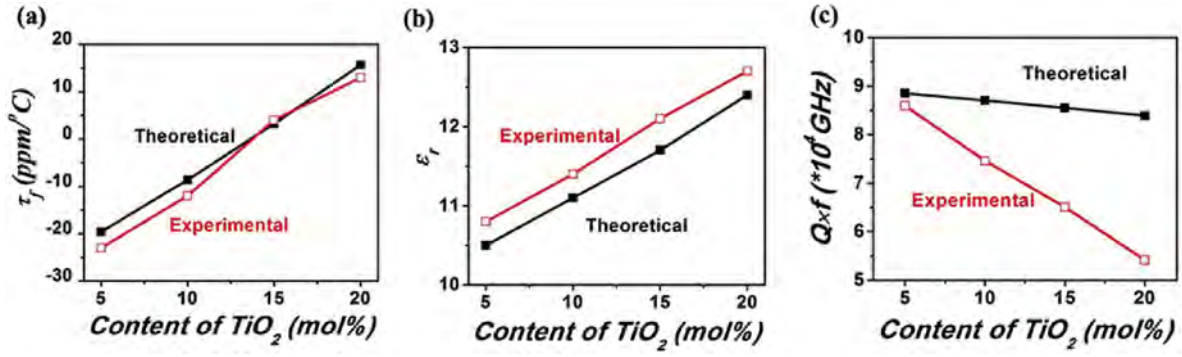

Fig. 11. Microwave dielectric properties of $ZnGa_2O_4$-TiO_2 composite ceramics sintered at 1300 °C for 2 h in air. (a) The experimental and theoretical temperature coefficient (τ_f); (b) The experimental and theoretical dielectric constant (ε_r); (c) Experimental and theoretical quality factors ($Q \times f$).

experimental ε_r value of $ZnGa_2O_4$-TiO_2 composite ceramics. The ε_r value of $0.85ZnGa_2O_4$-$0.15TiO_2$ is 12.

The theoretical $Q \times f$ value of $ZnGa_2O_4$-TiO_2 composite ceramics was obtained according to the formula: $Q^{-1} = v_1 Q_1^{-1} + v_2 Q_2^{-1}$, where v_1, v_2 are the volume fraction, and Q_1, Q_2 are quality factor of $ZnGa_2O_4$ ($Q_1 = 90{,}000$) and TiO_2 ($Q_2 = 51{,}000$), shown in Fig. 11(c). Due to the smaller Q_2, the theoretical $Q \times f$ value declined with the TiO_2 content. The experimental $Q \times f$ value shows the same trend as the theoretical value. Due to its highly sensitivity to microstructure and relative density, the difference between the calculated and experimental $Q \times f$ value became larger and large.

4. Conclusions

(1-x)$ZnGa_2O_4$-$xTiO_2$ ($x = 0.05$, 0.10, 0.15, 0.20) ceramics were successfully prepared by the conventional solid-state method. No side reaction existed during preparation. Introducing TiO_2 can effectively reduce the sintering temperature of $ZnGa_2O_4$ from 1400 °C to 1300 °C. The grain growth was promoted as well. The highest relative density was obtained at 1300 °C for each composition.

The theoretical and experimental data of ε_r, τ_f and $Q \times f$ were compared and show good consistent. Tunable microwave dielectric performance was achieved due to the compositing effect of TiO_2, especially for τ_f and $Q \times f$. τ_f value shifts from negative (−70 ppm/°C) to positive (+13 ppm/°C). Due to the inhomogeneous microstructure, the difference of $Q \times f$ value between calculated and experimented becomes larger and larger with increasing of TiO_2 content. $0.85ZnGa_2O_4$-$0.15TiO_2$ sintered at 1300 °C for 2 h, exhibits good microwave dielectric properties: $\varepsilon_r = 12.3$, $Q \times f = 73{,}000$ GHz, $\tau_f = +3$ ppm/°C. This work demonstrates that $ZnGa_2O_4$-TiO_2 composites are nice microwave dielectric ceramics with relative low sintering temperature, low dielectric constant, high quality factor, and near zero temperature coefficient. Moreover, it also provides a good example of rational design to tailor temperature coefficient.

Conflicts of interest

The authors declare that they have no conflict of interest.

Acknowledgements

This work was supported by Priority Academic Program Development of Jiangsu Higher Education Institutions (PAPD), the Opening Project of the State Key Laboratory of High Performance Ceramics and Superfine Microstructure (project No. SKL201309SIC), the College Industrialization Project of Jiangsu Province (JHB2012-12), the Jiangsu Collaborative Innovation Center for Advanced Inorganic Function Composites, the Science and Technology Projects of Guangdong Province (project No.2011A091103002), Graduate student training innovation project in Jiangsu province (KYCX17_0973), and China Scholarship Council (No. 201808320360).

References

[1] W. Wersing, Microwave ceramics for resonator and filters, Curr. Opin. Solid State Mater. Sci. 1 (1996) 715–731.
[2] R.J. Cava, Dielectric materials for applications in microwave communications, J. Mater. Chem. 11 (2000) 54–62.
[3] M.T. Sebastian, Dielectric materials for wireless communication, J. Mater. Chem. 11 (2010) 54–62.
[4] S.B. Narang, S. Bahel, Low loss dielectric ceramics for microwave applications: a review, J. Ceram. Process. Res. 11 (2010) 316–321.
[5] Z. Fu, P. Liu, J. Ma, X. Zhao, H. Zhang, Novel series of ultra-low loss microwave dielectric ceramics: $Li_2Mg_3BO_6$, (B = Ti, Sn, Zr), J. Eur. Ceram. Soc. 36 (2016) 625–629.
[6] D.X. Zhou, R.G. Sun, S.P. Gong, Y.X. Hu, Low-temperature sintering and microwave dielectric properties of 3Z2B glass–Al_2O_3 composites, Ceram. Int. 37 (2011) 2377–2382.
[7] S.H. Yoon, D.W. Kim, S.Y. Cho, K.S. Hong, Investigation of the relations between structure and microwave dielectric properties of divalent metal tungstate compounds, J. Eur. Ceram. Soc. 26 (2006) 2051–2054.
[8] A. Kan, H. Ogawa, H. Ohsato, S. Ishihara, Effects of variations in crystal structure on microwave dielectric properties of Y_2BaCuO_5 system, J. Eur. Ceram. Soc. 21 (2001) 2593–2598.
[9] Y.C. Chen, M.Z. Weng, J.M. Hong, Effect of Zr substitution on microwave dielectric properties of Zn_2SnO_4 ceramics, Ceram. Int. 25 (2014) 5000–5005.
[10] Y.C. Chen, Y.N. Wang, C.H. Hsu, Elucidating the dielectric properties of Mg_2SnO_4 ceramics at microwave frequency, J. Alloys Compd. 509 (2011) 9650–9653.
[11] N.H. Nguyen, J.B. Lim, S. Nahm, et al., Effect of Zn/Si ratio on the microstructural and microwave dielectric properties of Zn_2SiO_4 ceramics, J. Am. Ceram. Soc. 90 (2007) 3127–3130.
[12] W. Lei, W.Z. Lu, D. Liu, et al., Phase evolution and microwave dielectric properties of (1−x)$ZnAl_2O_4$−xMg_2TiO_4, ceramics, J. Am. Ceram. Soc. 92 (2009) 105–109.
[13] S. Takahashi, A. Kan, H. Ogawa, Microwave dielectric properties and crystal structures of spinel structured $MgAl_2O_4$ ceramics synthesized by a molten-salt method, J. Eur. Ceram. Soc. 37 (2016) 1001–1006.
[14] X. Chen, H. Xue, Z.H. Li, L. Wu, X.X. Wang, X.Z. Fu, Ternary wide band gap p-block metal semiconductor $ZnGa_2O_4$ for photocatalytic benzene degradation, J. Phys. Chem. C 112 (2008) 20393–20397.
[15] T. Ohtake, N. Sonoyama, T. Sakata, Luminescence dependence on imposing $ZnGa_2O_4$ activated with Mn^{2+} or Cr^{3+} n-type bias for $ZnGa_2O_4$ and semiconductor electrodes, Electrochem. Commun. 7 (2005) 1389–1392.
[16] Y. Zhuang, J. Ueda, S. Tanabe, Enhancement of red persistent luminescence in Cr^{3+}-doped $ZnGa_2O_4$ phosphors by Bi_2O_3 codoping, Appl. Phys. Express. 6 (2013) 2602.
[17] X.N. Zhang, J.H. Huang, K.N. Ding, Y.D. Hou, X.C. Wang, X.Z. Fu, Photocatalytic decomposition of benzene by porous nanocrystalline $ZnGa_2O_4$ with a high surface area, Environ. Sci. Technol. 43 (2009) 5947–5951.
[18] J. Xue, S. Wu, J. Li, Synthesis, Microstructure, and microwave dielectric properties of spinel $ZnGa_2O_4$ ceramics, J. Am. Ceram. Soc. 96 (2013) 2481–2485.
[19] S.P. Wu, J.J. Xue, R. Wang, J.H. Li, Synthesis, characterization and microwave dielectric properties of spinel $MgGa_2O_4$, ceramic materials, J. Alloys Compd. 585 (2014) 542–548.
[20] M.J. Lu, X. Ouyan, S.P. Wu, R.Y. Ge, R. Xu, A facile hydrothermal route to self-assembled $ZnGa_2O_4$ particles and their microwave application, Appl. Surf. Sci. 364 (2016) 775–782.
[21] M.M. Can, G.H. Jaffari, S. Aksoy, S.I. Shah, T. Firat, Synthesis and characterization of $ZnGa_2O_4$ particles prepared by solid state reaction, J. Alloys Compd. 549 (2013) 303–307.
[22] A. Kan, S. Takahashi, T. Moriyama, H. Ogawa, Influence of Zn substitution for Mg on microwave dielectric properties of spinel-structured (1-x)$MgGa_2O_4$-x$ZnGa_2O_4$, Jpn. J. Appl. Phys. 53 (2014), 09PB03.
[23] X.C. Lu, W.J. Bian, Y.Y. Li, H.K. Zhu, Z.X. Fu, Q.T. Zhang, Cation distributions and microwave dielectric properties of Cu-substituted $ZnGa_2O_4$, spinel ceramics, Ceram. Int. 43 (2017) 13839–13844.
[24] S. Takahashi, A. Kan, H. Ogawa, Microwave dielectric properties and cation distributions of $Zn_{1-3x}Al_{2+2x}O_4$ ceramics with defect structures, J. Eur. Ceram. Soc. 37 (2017) 3059–3064.
[25] X.C. Lu, W.J. Bian, Y.Y. Li, H.K. Zhu, Z.X. Fu, Q.T. Zhang, Influence of inverse spinel structured $CuGa_2O_4$ on microwave dielectric properties of normal spinel $ZnGa_2O_4$ ceramics, J. Am. Ceram. Soc. 101 (2017) 1646–1654.
[26] X.C. Lu, W.J. Bian, C.F. Min, Z.X. Fu, Q.T. Zhang, H.K. Zhu, Cation distribution of high-performance Mn-substituted $ZnGa_2O_4$ microwave dielectric ceramics, Ceram. Int. 44 (2018) 10028–10034.
[27] S. Zhang, H. Sahin, E. Torun, et al., Fundamental mechanisms responsible for the temperature coefficient of resonant frequency in microwave dielectric ceramics, J. Am. Ceram. Soc. 100 (2017) 1508–1516.
[28] D.W. Kim, B. Park, J.H. Chung, K.S. Hong, Mixture behavior and microwave dielectric properties in the low-fired TiO_2–CuO system, Jpn. J. Appl. Phys. 39 (2000) 2696.
[29] C.L. Huang, J.J. Wang, C.Y. Huang, Microwave dielectric properties of sintered alumina using nano-scaled powders of alumina and TiO_2, J. Am. Ceram. Soc. 90 (2007) 1487–1493.
[30] Y. Ohishi, Y. Miyauchi, H. Ohsato, K.I. Kakimoto, Controlled temperature coefficient of resonant frequency of Al_2O_3-TiO_2 ceramics by annealing treatment, Jpn. J. Appl. Phys. 43 (2004) L749–L751.
[31] X.C. Fan, X.M. Chen, X.Q. Liu, Complex-permittivity measurement on high-Q materials via combined numerical approaches, IEEE Trans. Microw. Theory 53 (2005) 3130–3313.
[32] J.Q. Yan, G.J. Wu, N.J. Guano, L.D. Li, Z.X. Li, X.Z. Cao, Understanding the effect of surface/bulk defects on the photocatalytic activity of TiO_2: anatase versus rutile, Phys. Chem. Chem. Phys. 26 (2013) 10978–10988.
[33] R.J. Wiglusz, A. Watras, M. Malecka, P.J. Deren, R. Pazik, Structure evolution and up-conversion studies of ZnX_2O_4: Er^{3+}/Yb^{3+} (X = Al^{3+}, Ga^{3+}, In^{3+}) nanoparticles, Eur. J. Inorg. Chem. 6 (2014) 1090–1101.
[34] S.P. Wu, J.J. Xue, R. Wang, J.H. Li, Synthesis, characterization and microwave

dielectric properties of spinel $MgGa_2O_4$ ceramic materials, J. Alloys Compd. 585 (2014) 542–548.
[35] M.M. Ba-Abbad, A.A.H. Kadhum, A.B. Mohamad, M.S. Takriff, K. Sopian, Synthesis and catalytic activity of TiO2 nanoparticles for photochemical oxidation of concentrated chlorophenols under direct solar radiation, Int. J. Electrochem. Sci. 7 (2012) 4871–4888.